Journal of Power Sources 228 (2013) 281–293

Contents lists available at SciVerse ScienceDirect

Journal of Power Sources

journal homepage: www.elsevier.com/locate/jpowsour

Systems for peaking power with 100% CO_2 capture by integration of solid oxide fuel cells with compressed air energy storage

Jake Nease, Thomas A. Adams II *

Department of Chemical Engineering, McMaster University, 1280 Main Street West, Hamilton, Ontario, Canada L8S 4L7

HIGHLIGHTS

- ► We model a novel CO_2 emission-free peaking power plant fueled by natural gas.
- ► Performance of different plant configurations are compared using defined metrics.
- ► Peaking power via CAES is possible with marginal impact on cost and efficiency.
- ► Partial shutdown for maintenance can be made while meeting demand and saving fuel.
- ► Proposed Plant becomes economically optimal at high fuel and carbon prices.

GRAPHICAL ABSTRACT

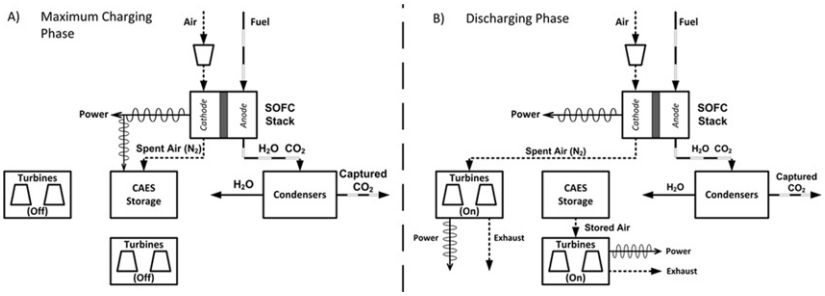

ARTICLE INFO

Article history:
Received 3 July 2012
Received in revised form
25 October 2012
Accepted 24 November 2012
Available online 1 December 2012

Keywords:
Solid oxide fuel cell
Compressed air storage
Carbon capture
Peaking power
Natural gas

ABSTRACT

In this study, the applicability and performance of an integrated solid oxide fuel cell (SOFC) and compressed air energy storage (CAES) plant with and without carbon capture and sequestration (CCS) in a load-following power production scenario is investigated. Ten different process configurations are simulated using a combination of Aspen Plus 2006.5 and MATLAB tools. It was found that the addition of CAES to an SOFC plant provided significant load-following capabilities with relatively small penalties to efficiencies (1.1%HHV) and levelized costs of electricity (LCOE) (0.08–0.3 ¢ kW^{-1} h^{-1}). The load-following capabilities of the CAES-enabled plants, as measured by proposed squared-error based metrics, were excellent and were not impacted by the addition of CCS. CCS-enabled configurations using SOFCs with and without CAES are able to reduce direct CO_2 emissions to essentially zero. The introduction of a seasonal, partial power train shutdown schedule, while useful for maintenance and cleaning purposes, also reduces fuel consumption by 9.5% with very small penalties to the overall load-following performance of the SOFC/CAES plant. Although SOFCs are perhaps decades away from being implemented on the scale discussed in this study, the forward-looking energy conversion strategy proposed in this work shows promise for providing future carbon-free peaking power.

1. Introduction

In most parts of the world, power production largely depends on the use of fossil fuels. Although efforts to utilize renewable energy sources such as solar, wind, and bio-fuels are ongoing, they currently only constitute a small portion of the energy portfolio due to cost and technical limitations. For the near term, it is desirable to maximize the efficiencies of current fossil-based power generation technologies, while remaining cognizant that carbon capture and control requirements may become a reality in the near future, likely driven by a carbon tax or emissions restriction. Consequently,

* Corresponding author. Tel.: +1 905 525 9140 x24782.
E-mail address: tadams@mcmaster.ca (T.A. Adams).

0378-7753/$ – see front matter © 2012 Elsevier B.V. All rights reserved.
http://dx.doi.org/10.1016/j.jpowsour.2012.11.087

industries that consume fossil fuels (such as electricity providers) may be required to capture the CO_2 generated by their operations and sequester it in underground spaces such as depleted oil fields, aquifers, and other geological storage sites [1]. As such, industries utilizing fossil fuels will be faced with the decision to either invest in the capture and sequestration of CO_2, or face the potential financial penalties associated with its emission.

With the above scenario in mind, this work investigates the combinatory effectiveness of an integrated solid oxide fuel cell (SOFC) and compressed air energy storage (CAES) plant for following demand-fluctuations (known as "peaking power") with and without CO_2 capture techniques enabled. Furthermore, the designs are also compared to a common natural gas-fed power process, the natural gas combined cycle (NGCC).

1.1. Natural gas combined-cycle plants

Natural gas-fed processes account for approximately 24% of all electricity generated in the United States and is anticipated to rise to 27% by 2035. [2]. In Canada, natural gas accounts for 9% of the electricity generated and is projected to increase to 15% by 2035 [3]. Natural-gas fired power plants produce inherently lower emissions per unit of electrical energy than coal (50.29 g MJ^{-1} versus 90.29 g MJ^{-1}) [4], and therefore are responsible for a proportionally smaller amount of the CO_2 emissions in the power sector. For example, in the United States, natural gas contributes to only 17.5% of the carbon emissions for the electricity sector [2,5] while producing 24% of the power. However, the emissions from a standalone NGCC plant are still significant, and other approaches may be required to reduce the emissions of natural gas power plants to a sustainable level [7].

The NGCC process is briefly described as follows [6,8]: First, the natural gas fed to the plant is cleaned and desulphurized if it was not done so prior to distribution. The gas is then combusted in air at a high temperature and pressure in a gas turbine unit, which produces electricity through a generator attached to the turbine. The waste heat from the exhaust stream may then be recovered through the generation of high pressure steam, which can be used to power turbines in a steam cycle for additional power generation (hence the name "combined cycle"). The exhaust, which now contains mostly CO_2, water and nitrogen from the combustion step, may then be subjected to a solvent-based absorption process which serves to separate the CO_2 from the flue gas with approximately 90% recovery should carbon capture be desired. The CO_2 stream is then cooled and compressed to supercritical conditions suitable for transport in a CO_2 pipeline, and the decarbonized exhaust stream is vented to the atmosphere through a flue stack. However, a significant amount of energy is required for CO_2 capture in the NGCC process (up to 14% of the net power produced) which can cause up to a 40% increase in the levelized cost of electricity (LCOE) [8].

1.2. Solid oxide fuel cells

A solid oxide fuel cell (SOFC) utilizes a fuel gas and an oxidant (typically air) to efficiently produce electrical power through electrochemical reactions on opposite sides of a solid oxide barrier, as depicted in Fig. 1. The reactions that occur in the anode and cathode include:

$$H_2 + O^{=} \rightarrow H_2O + 2e^{-} \quad \text{(Anode)} \tag{1}$$

$$CO + O^{=} \rightarrow CO_2 + 2e^{-} \quad \text{(Anode)} \tag{2}$$

$$O_2 + 4e^{-} \rightarrow 2O^{=} \quad \text{(Cathode)} \tag{3}$$

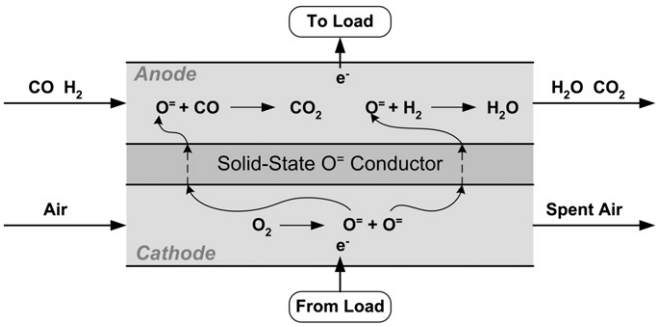

Fig. 1. Simple schematic of an SOFC using syngas as a fuel source as investigated in this study.

In addition to hydrogen gas and carbon monoxide (the two of which comprise synthesis gas or "syngas"), other suitable fuel sources for the SOFC anode include natural gas [9] and methanol [10] which can be used directly in the anode. Moreover, fuels such as coal [11], diesel [10], ethane and even biomass [12] can be pre-processed into syngas and used as a fuel source. Provided that the fuel utilization is high and the SOFC is equipped with appropriate seals that maintain separation between the anode and cathode exhausts, the anode exhaust will consist mainly of H_2O and CO_2. The anode exhaust can hence be separated relatively easily, and the resulting captured CO_2 can be compressed for pipeline transport. The cathode exhaust is partially deoxygenized air at high temperatures ($\sim$900 °C), which can be used for additional power generation through heat recovery and vented without posing an environmental risk. If the SOFC is operated at high pressures (10–20 bar), electricity can also be generated by feeding the hot, pressurized cathode exhaust to a gas turbine, thus forming a Brayton cycle. Our prior work has shown that pressurized SOFC systems of this type are capable of generating power at high efficiencies (up to 74% by higher heating value) with essentially no CO_2 emissions [6]. Comparable studies by other groups have found similar results [28,30]. Furthermore, the process of electrochemical energy conversion to electricity is more efficient than combustion, which allows the SOFC plant to achieve higher thermal efficiencies than systems that utilize the Carnot cycle.

However, one significant disadvantage of SOFC systems is that there are currently potentially cost-prohibitive operability challenges associated with their dynamic operation. For example, it is possible to change the power output of an SOFC relatively quickly (for example, in response to load changes) [13], but this runs the risk of very high degradation rates or even destruction due to rapid thermal expansion or the backflow of gases [14]. To avoid these risks, it is probable that future large-scale SOFCs will operate at a fixed power output which will not be adjusted to follow the typical diurnal power demand profile of a typical power grid. Of course, a system with a fixed power output can be scaled large enough to always meet demand, but this approach would be wasteful since it would almost always produce more electricity than necessary.

1.3. Compressed air energy storage

Compressed Air Energy Storage (CAES) plants operate as an intermittent source or sink for electrical power. The plant consumes power in order to compress air to high pressures and store it in an either man-made or naturally occurring void (which may be above- or below-ground) as elastic potential energy. During periods of high power demand or electricity prices, the stored compressed air

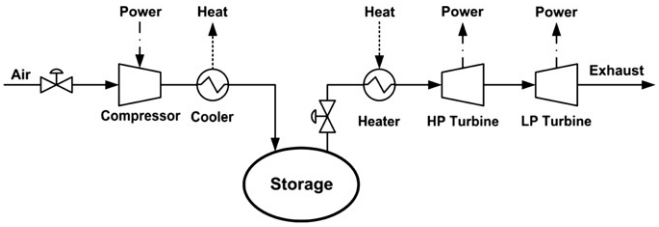

Fig. 2. Simplified CAES system schematic [23].

is pre-heated (usually by combusting natural gas) and fed to gas turbines attached to an electric generator, thereby re-supplying the stored energy back to the power grid. A simplified schematic of a typical CAES system is shown in Fig. 2.

CAES technology has been utilized for over three decades. The Alabama Electric Corporation has been operating a 110 MW plant since 1991, and E.N. Kraftwerke has been running a 290 MW plant in Huntorf, Germany since 1978 [15]. There have been several other studies and plans to construct further CAES plants in North America, but at the time of this publication no others have been constructed to the best of our knowledge [16].

CAES is advantageous for a variety of purposes; not only can it serve as a stand-alone plant capable of achieving profitability through compressing at times of low electricity prices and releasing at times of high prices, but it can also be combined with other processes to add flexibility or reliability. For example, there has been significant theoretical research in recent years examining the utilization of CAES as a method for leveling intermittent sources (such as wind power) to provide a consistent base load [15,17–22]. However, there has not been much research concerning the integration of CAES with other power sources for the purposes of load following (or "peaking").

1.4. SOFC/CAES integration concept

In order to provide reliable, peaking power with 100% CO_2 capture, we propose the integration of SOFCs (to provide base-load power), a CCS system (to achieve near-zero CO_2 emissions), and a CAES system (to following peaking demand). The SOFC and CCS systems used are modeled after the prior work of Adams and Barton (2010) [6] but modified to incorporate CAES. During the night or periods in which demand is low, the CAES system can be used to charge the available storage space in which a portion of the electrical power generated by the SOFC system is used to compress some or all of the cathode exhaust to the current pressure of the underground storage cavern. The portion of the cathode exhaust which is not sent to CAES is sent to a turbine attached to a generator to produce additional electricity, as shown in Fig. 3(A). During times when the electricity demanded is high, all of the cathode exhaust is sent to the gas turbine, maximizing the electricity produced by the SOFC/GT system. In addition, air is released from the storage space and fed to a second gas turbine system, producing additional power, as expressed in Fig. 3(B). A more detailed PFD of the proposed integrated process is provided in Fig. 4, and a detailed description of the process and its model is given in Section 2.

With this approach, the proposed SOFC/CAES/CCS system is able to provide load-following power from fossil fuels while maintaining high efficiency capturing nearly 100% of the CO_2. Because the system does not use SOFCs in load-following mode, there is a significantly lower risk of damage or shortened lifetime compared to using SOFCs in a load-following mode, as mentioned in Section 1.2. Furthermore, the system allows for the generation of large amounts of power during brief periods significantly above the normal power output of the SOFCs thanks to the use of CAES. This means that SOFCs need only be large enough for the "average" power produced, instead of the largest expected peak value which occurs for only a short time.

In this work, a techno-economic analysis of several configurations of the integrated SOFC/CAES process is presented. Simulations are used to compute mass and energy flows using Aspen Plus v7.3 for steady-state computations and in-house models implemented in MATLAB for dynamic simulations. For the economic analysis, the historical power demand profile for the province of Ontario, Canada in 2011 [25] was considered. Details are presented in the next section.

2. Simulation models

Many process systems have been proposed which use SOFCs or SOFCs with gas turbines using natural gas as a fuel source [24–30] (a comprehensive review can be found in Adams et al. (2012) [23]). The SOFC system selected for this work is based on the system presented in Adams and Barton (2010) [6] using the same modeling and design assumptions for consistency. This was integrated with CAES to form the proposed integrated SOFC/CAES process presented in Fig. 4. The SOFC system may be divided into the following sections, each discussed in turn: reforming, gas shifting, power generation, heat recovery and steam generation (HRSG), and CO_2 recovery. The CAES system may be divided into two sections, namely compression and storage, and expansion.

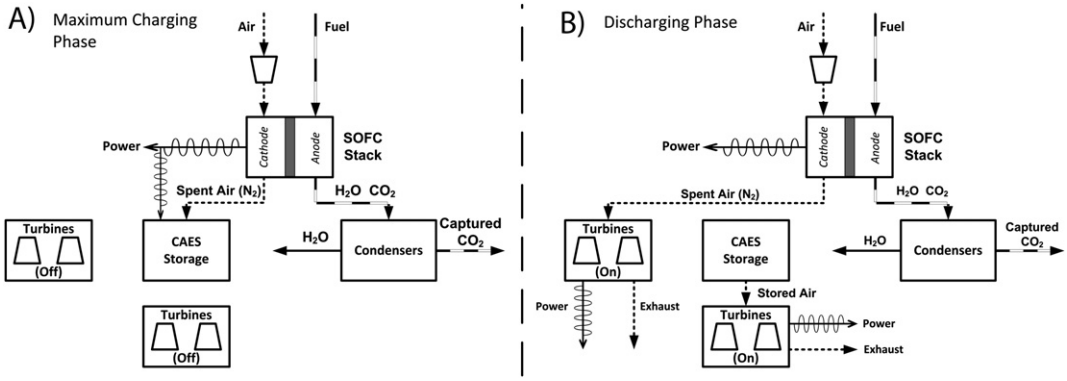

Fig. 3. Simplified SOFC/CAES integration technique during (A) the maximum charging phase, and (B) the discharging phase.

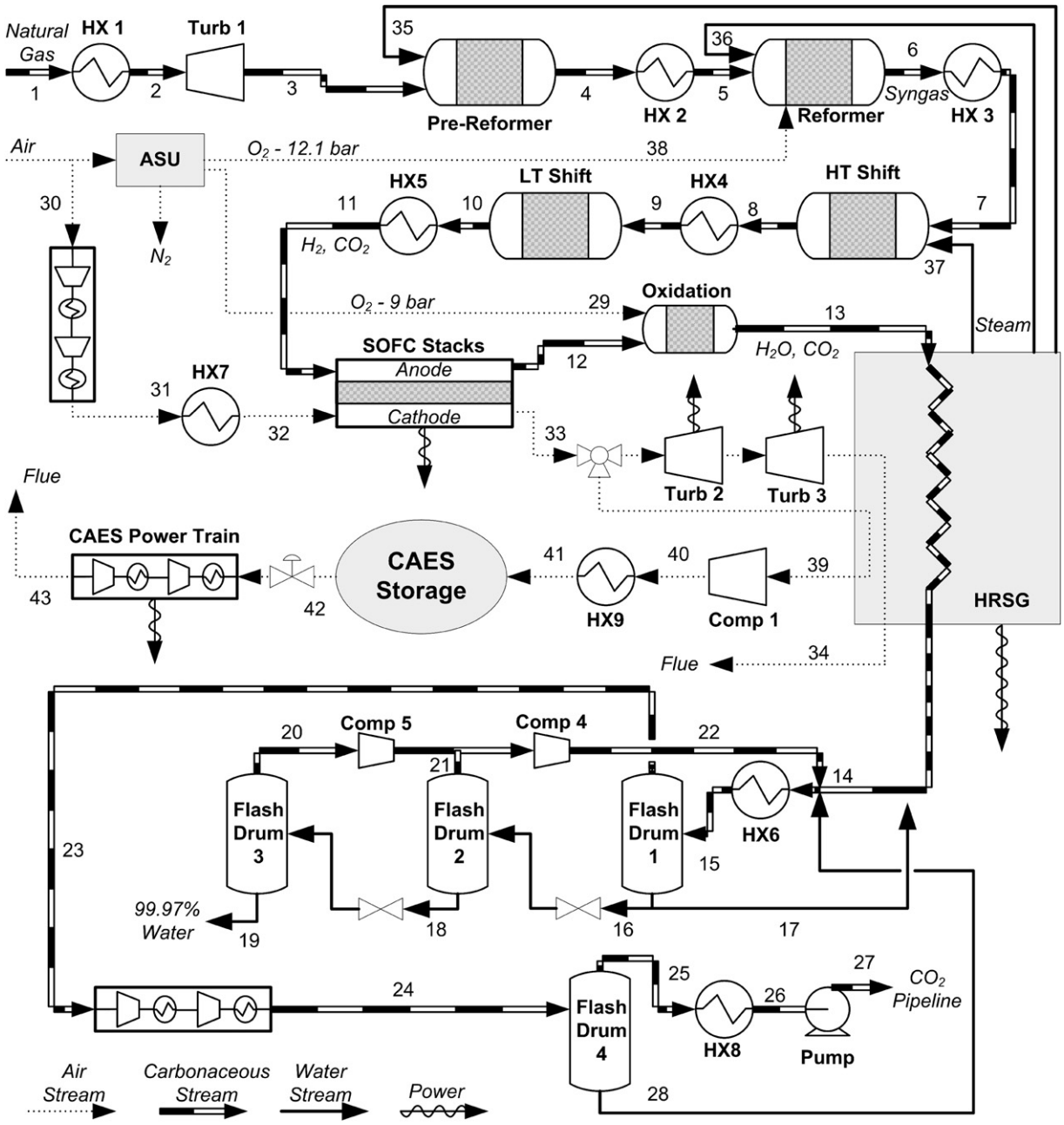

Fig. 4. PFD of proposed SOFC/CAES plant.

2.1. Basis of steady-state simulation and modeling approach

The SOFC plant examined in this study was modeled after that of the previous work, with a targeted base-load power output of 714.4 MW (including the net power produced by the SOFCs, the cathode Brayton cycle turbines 2 and 3, and the combined cycle in the HRSG). It should be noted that in the prior work, several process configurations were explored, and the configuration chosen for this paper is consistent with the configuration called the "autothermal reforming case" discussed therein [6]. The natural gas fed to the plant is assumed to be supplied at 30 bar and 38 °C and contains 93.9 mol% methane, 3.2% ethane, 0.7% propane, 0.4% *n*-butane, 1% CO_2 and the remainder N_2 [6]. Simulations of the SOFC/CAES plant were performed using Aspen Plus 2006.5 with the Peng–Robinson equation of state (EOS) including the Boston-Mathias modification throughout, except that the Redlich–Kwong–Soave EOS with predictive Holderbraum mixing rules was used for streams containing mostly CO_2 and H_2O below the critical point of CO_2, and the electrolyte-NRTL model with Henry coefficients and electrolyte specifications from the AP065 databank for H_2O/CO_2 streams near the critical pressure of CO_2. For sample stream conditions for a slightly different configuration of the SOFC plant, the reader is referred to the previous study [6].

2.2. Solid oxide fuel cell process and model

2.2.1. Natural gas reforming and syngas shifting

The reforming of natural gas involves its reaction with steam at temperatures above 700 °C to produce syngas through the following chemical reactions:

$$C_nH_m + nH_2O \leftrightarrow nCO + (0.5m + n)H_2 \quad (4)$$

In order to obtain high conversions (up to 99%) of this reaction at high pressures, very high temperatures are required (as high as 1000 °C at 15 bar pressure) [31]. The water-gas-shift (WGS) and CO_2 reforming reactions may also take place at these temperatures and pressures, leading to different overall yields of the desired H_2 and CO products [32]:

$$CO + H_2O \leftrightarrow CO_2 + H_2 \quad (5)$$

$$CH_4 + CO_2 \leftrightarrow 2CO + 2H_2 \quad (6)$$

It is possible to design the SOFC system such that natural gas reforming can take place inside the anode of the SOFC due to its high operating temperature and pressure (called "internal" natural gas reforming). Although this can be advantageous for reasons of thermal management (the endothermic reforming reaction can be used to regulate the exothermic electrochemical reaction in the fuel cell), there could be problems with carbon deposition and fouling inside the anode leading to serious challenges associated with the long-term operability of an internally-reforming fuel cell stack [33–35]. Although the most recently introduced commercial SOFCs use "internal" natural gas reforming (at the 1–200 kW stack scale) [23], it is unclear what configuration will be used at the megawatt scale since they are not yet commercially available. For example, "external" reforming may be preferred, in which natural gas is reformed (and possibly shifted) prior to entering the SOFC anode. In this work we consider the case where "external" reforming and gas-shifting are used (as shown in Fig. 4) in order to be consistent with the prior work. Although the external and internal reforming configurations will have some differences in cost and performance, the balance of the SOFC/CAES process is essentially the same regardless of the reforming and shifting strategy chosen.

In the process proposed in this work, natural gas is pre-heated to 615 °C and expanded to 12.5 bar through a turbine. The expanded gas is then sent to a pre-reformer, where the conversion of C_nH_m for $n > 1$ is assumed to be 99.9%. Reforming of C_nH_m where $n = 1$ as well as all side reactions are assumed to reach equilibrium. The pre-reformer effluent is then sent to an autothermal reformer (ATR) where restricted oxygen supplied from an air separation unit (ASU) at 92 mol% purity is used to oxidize a small portion of the remaining methane, generating the necessary heat to simultaneously reform the remaining methane with steam. The detailed design of the pre-reformer and ATR operating conditions are discussed in the previous work [6].

The syngas produced by the reforming section is reacted via the WGS reaction given in equation (5). The ATR effluent is sent to two plug-flow reactors in series. The first reactor operates at a high temperature (300–350 °C) and is assumed to achieve an 80% conversion of CO; the second reactor operates at a lower temperature (200–250 °C) and approaches equilibrium, therefore achieving an overall conversion of approximately 96% [8]. Details are available in the prior work [6].

2.2.2. Power generation and heat recovery

The SOFC generates electrical power through reactions (1) through (3). The SOFC stacks operate at a pressure of 10.1 bar and a temperature of approximately 950 °C. Although higher efficiencies are possible when higher temperatures are used, material limitations usually prevent the SOFC from surpassing 1000 °C [36]. The shifted syngas leaving the WGS unit is pre-heated to 910 °C, and fed to the anode of the fuel cell stack. Ambient air is compressed and heated to the same conditions and fed to the cathode. The anode and cathode exhaust streams are kept separate to prevent the mixing of N_2 and CO_2, allowing for cost-effective CO_2 capture and sequestration (see Section 2.2.3). The anode exhaust is fed to an oxidization unit where the unreacted H_2 and CO are completely oxidized with oxygen at 92 mol% purity (from the ASU) to H_2O and CO_2. The actual SOFC stacks were modeled using the same methods as in the prior work, where the achieved potential from a given cell is temperature and pressure dependant as described in Ref. [36].

The proposed design includes six parallel SOFC power generation trains of equal size, for several reasons. First, having multiple SOFC trains will allow for continued operation of the plant at 5/6 capacity should a malfunction in one train occur. Second, routine shutdowns of a particular stack may be scheduled for maintenance purposes (de-coking, re-sealing, replacement of electrical equipment, etc.). Finally, when incorporating the CAES design, it is possible to save fuel while still meeting demand by allowing for seasonal shutdowns of certain trains.

In the proposed SOFC/CAES system, the cathode exhaust may travel through one of two possible routes. During periods of low demand, all or a portion of the cathode exhaust stream is routed to a compressor that compresses it to the appropriate pressure in order to charge the CAES storage space. However, during periods of high demand the cathode exhaust is expanded to atmospheric pressure through a series of turbines to generate additional power. In both cases, the thermal energy contained after compression or expansion is recovered in the HRSG to improve thermal efficiency.

The design considerations of the HRSG and its associated heat exchanger network (HEN) are similar to the previous work [6] and are not discussed in this work. The two main assumptions made in modeling the HRSG are: (1) the HEN avoids temperature crossover but assumes an ideal ΔT_{min} of 0 °C for the sake of simplicity, and (2) all waste heat between 50 and 950 °C may be used as a heat source for the steam cycle, which contains 5 steam pressure levels.

2.2.3. CO_2 recovery

After heat recovery, the anode exhaust (containing mostly CO_2 and H_2O) is separated by a series of cascading flash drums as described by Adams and Barton (2010b) [37]. Some of the high purity water is fed to the HRSG to generate steam for other parts of the process, and the excess water from the final flash drum may be treated and used for other purposes. The CO_2 rich vapor is compressed to 74 bar (near the critical point) and flashed once more to remove most of the remaining water and achieve the CO_2 purity required for pipeline transit. The CO_2 stream is condensed to a liquid and pumped to 153 bar before it leaves the plant, destined for CO_2 sequestration.

2.3. Compressed air energy storage process and model

The CAES section was partially modeled in Aspen Plus. Design and operating parameters of the CAES process are given in Table 1. After leaving the SOFC, the cathode exhaust is split depending on the amount desired to be stored at that time (details on dynamic simulations will be provided in the following sections). The exhaust diverted to the CAES compression section is cooled to a temperature suitable for the compressor inlet (assumed to be 50 °C) via the HRSG. The stream is then compressed to a pressure between 42 and 72 bar (to reach a pressure 2 bar above the current air pressure within the cavern), and finally is cooled to 50 °C before being injected into the storage cavern. It is assumed that all of the heat recovered from cooling the compressed exhaust can be effectively recovered and used in the HRSG for the production of various grades of steam and heated water. The equipment selection for the CAES compression section was based on the heuristics provided by Luyben (2011) [38] as well as the Huntorf plant model developed by Raju and Khaitan (2012) [15]. It is also assumed that, once the storage air has entered underground storage cavern at

Table 1
Operating characteristics the CAES section of the proposed SOFC/CAES integrated system.

Operating condition	Value	Units
Air turbines (CAES power train in Fig. 4)		
Rated turbine power	200	MW
Maximum air flow rate	440	kg s^{-1}
Inlet pressure to HP turbine	40	bar
Inlet temperature to HP turbine	550	°C
Inlet pressure to LP turbine	6	bar
Inlet temperature to LP turbine	825	°C
Turbine efficiency	75	%
Compressor (Comp 1 in Fig. 4)		
Maximum air flow rate	210	kg s^{-1}
Rated compressor power	140	MW
Temperature at exit of after-cooler	50	°C
Pressure at exit of after-cooler	42–73	bar
Compressor isentropic efficiency	75	%
Cavern		
Volume of storage space	600,000	m^3
Cavern operating pressures	40–72	bar
Maximum cavern pressure	72	bar
Cavern wall temperature	50	°C

a temperature of 50 °C, there is negligible heat transfer between the stored air and the cavern walls [39] and the cavern is therefore considered to be isothermal. The CAES storage cavern is assumed to be a solution-mined salt dome with a volume of 600,000 m^3, which is comparable in size to the Huntorf plant [15]. The temperature changes due to friction by the transport to and from the storage cavern via the injection/withdrawal wells were calculated using the VALVE model in Aspen Plus and found to be on the order of 1 °C. Therefore, this temperature change was neglected for simplicity.

When the CAES cavern is to be discharged, all of the cathode exhaust is sent to turbine 2 and none is sent to the cavern (see Fig. 4). As such the power produced by turbines 2 and 3 are at their maximum level. The stored cathode exhaust in the CAES cavern is released at a rate depending on the desired total net power output of the integrated SOFC/CAES plant. The stored cathode exhaust is throttled to 40 bar with a valve, pre-heated to 550 °C and expanded through high- and low-pressure turbines, generating as much as 200 MW of power beyond the base-load of 714 MW (28%). It should be noted that the temperature losses across the valve were calculated using Aspen Plus and found to be at most 5 °C, which has very little impact on the overall performance of the CAES plant, and therefore was neglected for simplicity.

2.4. Dynamic simulation modeling approach

In order to simulate the SOFC/CAES plant dynamically while attempting to follow a transient load profile, the transient portions of the SOFC/CAES plant were modeled using a pseudo-steady-state approach. The transient portions included all units downstream of stream 33 (cathode exhaust Brayton cycle turbines, cathode exhaust compressors, the storage cavern, stored gas expansion, and related heat integration). In contrast, all units upstream of stream 33 (all natural gas processing, SOFCs, the CCS section, and related heat integration) are always steady-state and do not need to be considered in the pseuo-steady-state model.

Pseudo-steady-state Aspen Plus simulations of the transient portions of the plant were separated into two distinct modes of operation: charging and discharging of the CAES cavern. For each mode, a sensitivity analysis was run for a variety of cavern pressures and air flow rates to (in the charging mode) and from (in the discharging mode) the CAES cavern. These resulting data were regressed to multi-dimensional nonlinear equations in which the net power output of the plant (P_P, in MW) was the dependent variable. This yielded the following nonlinear pseudo-steady-state model to predict the power output of the combined SOFC/CAES plant:

$$P_P = I_M + a_{10}\frac{(F-\mu_F)}{\sigma_F} + a_{01}\frac{(P_C-\mu_{P_C})}{\sigma_{P_C}} + a_{20}\left(\frac{(F-\mu_F)}{\sigma_F}\right)^2 + a_{11}\frac{(F-\mu_F)}{\sigma_F}\frac{(P-\mu_{P_C})}{\sigma_{P_C}} + a_{02}\left(\frac{(P-\mu_{P_C})}{\sigma_{P_C}}\right)^2, \quad (7)$$

where I_M is the model intercept, F is the molar flow rate of air into the CAES storage cavern, P_C is the required pressure at the compressor outlet, a_{ij} is the model coefficient for the ith and jth power of F of P_C, respectively, and μ_k and σ_k are the arithmetic means and standard deviations where $k \in \{F, P_C\}$, respectively. Equation (8) may then be inverted in order to calculate the required flow rate to or from the cavern depending on the desired output of the plant at that time.

These resulting pseudo-steady-state models for the discharging and charging phases were programmed into MATLAB to allow for the dynamic calculation of the net output of the SOFC/CAES plant depending on the power demanded at any given time. Furthermore, the model anticipates the molar content and pressure of the CAES cavern at the end of each time step to ensure that they remain between the allowable operating ranges for the proposed system. The MATLAB calculation sequence is shown graphically in Fig. 5. For the purposes of the dynamic simulations in this study, 1-h control intervals were chosen for several reasons. Firstly, due to previous daily and seasonal power demand data, very accurate predictions of future power demand (up to 24 h in advance) are available [25]. Furthermore, the dynamics of CAES systems are limited only by the dynamics of the compressor and expansion turbines. A plant with one or more 135 MW generators can startup in 7–10 min, and ramp

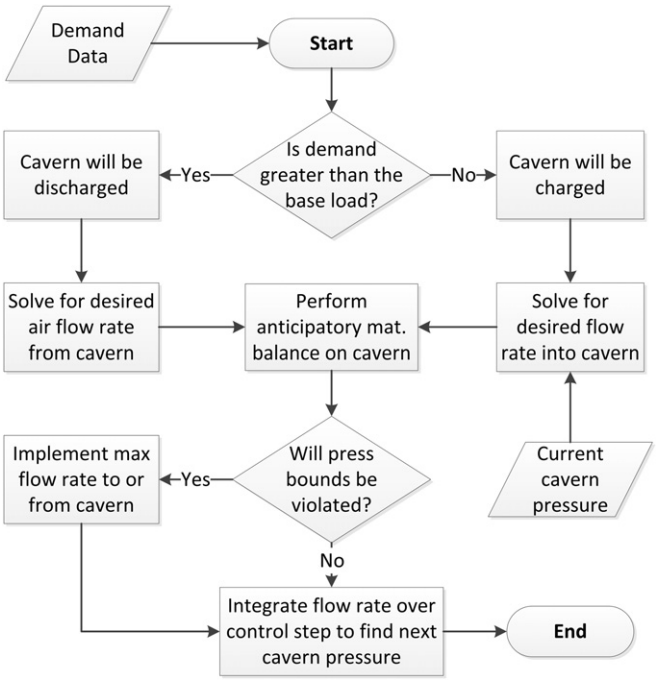

Fig. 5. MATLAB calculation sequence for a single simulation time step.

at approximately 4.5 MW per second (therefore requiring 30 s to obtain the maximum output) [40]. The CAES compressor starts in approximately 10–12 min and ramps at 20% per minute thereafter [16]. The dynamics of a CAES plant are therefore suitable for dynamic load-following, allowing for full operational changes in 15 min or less. With the above in mind, the dynamics associated with compressor and turbine adjustments as well as the actual control structure of the proposed plant is out of scope and was not considered in this study. Instead, it is assumed that the SOFC/CAES combined plant is capable of meeting the target power demand instantly at the beginning of each time step (1 h intervals), and therefore a pseudo-steady-state model is appropriate.

2.5. Combined plant scenario and operational objectives

The operational objective of the proposed SOFC/CAES plant in this study is to follow the power demanded as closely as possible over a year-long operational period. The effects of wear and tear during the lifetime of the plant are not considered. The scenario for this investigation is as follows: It is assumed that a plant must be constructed to meet the demand of a large (500–900 MW) community that exhibits a similar peaking profile (relative amplitude, frequency of peaks) to that of the actual grid demand for Ontario, Canada in 2011, scaled to an average of 714 MW [25]. Whenever the plant does not produce enough power to meet demand, it is assumed that the deficit is purchased from the grid at the current electricity price for that control interval (also from historical data for Ontario [25]). In addition to paying full price for the electricity purchased, it is assumed that the majority of the electricity obtained from the grid was produced by a natural gas-based peaking plant that emits 50.29 g of CO_2 equivalents per MJ of power produced [41]. Emissions from these grid-supplying plants are accounted for as indirect CO_2 emissions for each plant considered. It is further assumed that any excess power that is produced may be transmitted to the grid, but at no financial gain to the plant.

The metrics used to measure the performance of each plant configuration were the levelized cost of electricity (LCOE), the sum of squared-errors (SSE), and the weighted sum of squared-errors (WSSE) [43]:

$$\mathrm{LCOE} = \sum_{t=0}^{N}\left(\frac{\frac{I_t + M_t + \mathcal{F}_t}{(1+r)^t}}{\sum_{t=0}^{N}\frac{P_t}{(1+r)^t}}\right) \tag{8}$$

$$\mathrm{SSE} = \sum_{i=1}^{n}(P_{\mathrm{P},i} - D_i) \tag{9}$$

$$\mathrm{WSSE} = \sum_{i=1}^{n}\left[U_i^2 + \left(\frac{O_i}{2}\right)^2\right], \tag{10}$$

where in the LCOE calculation I_t, M_t, $\mathcal{F}_t$ and P_t are the capital expenditures, maintenance costs, fuel costs and total sellable power produced in year t, respectively. The plant lifetime is N years (20 years) and is discounted at a real interest rate of r (10%). The variable D_i represents the demand at interval i over n time steps (1 h per time step for one year). O_i is the amount of power over-produced by the plant and U_i is the amount under-produced by the plant at time step i.

The LCOE metric gives insight into the economic tractability, whereas the SSE and WSSE are meant to exhibit the load-tracking capabilities of each proposed plant configuration. The WSSE differs from the SSE in that WSSE does not fully penalize over-production; although this is wasteful from an operational standpoint, demand is fully met in this case and therefore is not penalized as much as underproduction.

2.6. Case studies

Ten different plant configurations have been simulated in order to compare their performance in the load-following scenario described in Section 2.5. Two cases are standard NGCC plants (with and without carbon capture and sequestration (CCS)), and eight cases are base-load SOFC power plants (also with and without CCS), both at fixed output of 714 MW. It is recognized that NGCC and other natural-gas fired power plants can sometimes have peaking capabilities, but according to the US Energy Information Administration: 'facilities that previously served peaking or more often intermediate load needs now contribute more significantly to base load electricity needs' [42]. The CCS method for the NGCC is solvent-based, and captures 90% of the CO_2 from the flue gas [6]. The remaining eight cases involve different configurations of the integrated SOFC/CAES plant with and without CCS and with and without the ability to shutdown one of the six SOFC trains on a seasonal basis. A summary of the features of each case is given in Table 2. The assumptions made with regards to the simulation and financial calculation parameters are provided in Table 3.

Train shutdown involves shutting down an SOFC train and reducing the process inlets proportionately to decrease the throughput of the plant for a period as long as several months. For this investigation, it is assumed that there are six SOFC process trains of equal size, and that the SOFC power generation section can operate at 5/6 capacity while one is shutdown. The assumptions about upstream operations reaching chemical equilibrium result in identical stream conditions (temperatures, pressures) upstream of the SOFC stacks. Thus no modeling changes to the units upstream of the SOFCs are required. A train shutdown not only allows for maintenance to be performed on the SOFC stacks, but also may be timed with seasonal decreases in demand to prevent unnecessary overproduction. Seasonal trends tend to show lower demand during the spring and fall and higher during the winter and summer [25]. The demand profile used in this study (shown as the average daily demand for improved readability) and the proposed train shutdown schedule are shown in Fig. 6. For this analysis, the proposed schedule was selected by manual inspection.

Capital cost estimates for the NGCC and SOFC plants were obtained using a combination of Aspen Icarus cost estimation software, published cost estimates, cost estimation methods provided by Seider et al. [44] and appropriate assumptions in order to be

Table 2
Description of simulated cases.

Case number	Tag	Base-load source	CCS enabled?	CAES enabled?	Train shutdown enabled?
1	NGCC	NGCC	No	N/A	N/A
2	NGCC–CCS	NGCC	Yes	N/A	N/A
3	SOFC	SOFC	No	No	No
4	SOFC–CCS	SOFC	Yes	No	No
5	SOFC–CAES	SOFC	No	Yes	No
6	SOFC–CAES–CCS	SOFC	Yes	Yes	No
7	SOFC–TSD	SOFC	No	No	Yes
8	SOFC–TSD–CCS	SOFC	Yes	No	Yes
9	SOFC–CAES–TSD	SOFC	No	Yes	Yes
10	SOFC–CAES–CCS–TSD	SOFC	Yes	Yes	Yes

Table 3
Assumed parameters for case studies.

Parameter	Value	Units[a]
Initial natural gas cost [47]	2.33	$ GJ^{-1}
HHV of natural gas [2]	52,970	kJ kg^{-1}
NG feed at full plant capacity (all 6 SOFC trains in service)	74,926	kg h^{-1}
NG feed at reduced plant capacity (only 5 SOFC trains in service)	62,436.4	kg h^{-1}
CO_2 tax[b]	50.00	$ tonne^{-1}
Plant lifetime	20	Years
Discount rate	10.0	%
Inflation rate	2.5	%

[a] Cost units are expressed in US$2007 using the Chemical Engineering Cost Index [49].
[b] This CO_2 tax is the "standard" for comparison, but is investigated in greater detail in Section 3.4.

consistent with the prior work [6]. The reader is referred to the prior work for details regarding the sizing, material selection and other assumptions with regards to the process costing step. The installed cost of an SOFC stack was assumed to follow a linear scaling profile of \$1000 kW^{-1}, and therefore the economy of scale penalties associated with using multiple, smaller power trains in parallel is already accounted for by this worst-case scaling assumption. The target for Fuel Cell Energy's SOFC stack costs in the year 2012 is \$496 kW^{-1} (US\$2007) and includes all of the appurtenances required for its operation [45], with other targets being even lower [46]. As such the estimate of \$1000 kW^{-1} is expected to be conservative for a mature plant [9]. CAES plant costs included the estimation of the injection/withdrawal wells, turbomachinery and storage cavern. The cost estimate for the storage cavern and its injection wells was obtained from Schainker (2009) [47] and assumes a linear cost \$1.5 MW^{-1} h^{-1} of storage. Turbomachinery costs were combined estimates of those from Mason (2012) [21], Seider [44], and Schainker (2009) [47]. Natural gas costs were assumed to begin at \$2.33 GJ^{-1} (\$2.46 MMBtu^{-1}) and then inflate at 2.5% per year over the lifetime of the plant [48].

3. Results and discussion

3.1. Overall system results and performance

A summary of the operational results for each case investigated is presented below in Table 4. The SOFC base-load plant has the highest efficiency of the configurations examined, and is consistent with the prior work [6]. Furthermore, the addition of the CAES component to the original base-load plant in both the CCS enabled and CCS disabled cases reduces the overall efficiency of each plant by approximately 0.6 percentage points due to losses from compression and throttling. The addition of CAES to any of the scenarios when train shutdown is enabled also decreases the overall efficiency of the plant by less than 1 percentage point in each case, although the addition of train shutdowns itself imposes a close to 1.1 percentage point decrease in efficiency largely due to lower attainable efficiencies in the HRSG. These results therefore indicate that, since the partially compressed cathode exhaust may be used as the energy storage medium, significant load-following capabilities may be introduced to an SOFC base-load plant in the form of CAES with a small reduction in plant efficiency.

The introduction of CCS has a large impact on the direct CO_2 emissions for each case, with complete capture for the SOFC base-load plant with CCS enabled. Furthermore, the introduction of train shutdowns decreases the direct natural gas consumed over the year and as such decreases the amount of direct CO_2 sequestered (in the CCS cases) or emitted (in the non-CCS cases). However, the introduction of train shutdowns also increases the amount of external grid power that must be purchased in order to meet demand, thereby increasing the indirect CO_2 emissions for the train shutdown cases. This leads to the interesting result that even though there is less direct fuel consumption by cases in which CAES and SOFC train shutdown are enabled, the indirect CO_2 emissions for these plants is higher than the SOFC cases where train shutdowns are not performed. For example, case 9, the integrated SOFC/CAES with train shutdowns (TSD) case, consumes approximately 9.5% less natural gas (directly) than the case in which a baseline SOFC plant is used without CAES or train shutdowns (case 3), but also produces 36% more indirect CO_2 emissions to meet the same peaking demand profile. However, the total CO_2 emissions (direct plus indirect) of case 9 are about 8.3% lower than case 3. This means that even though using CAES and train switching requires more external grid power, the total lifecycle CO_2 emissions are reduced by about 8.3%. In addition, case 9 has an advantage that by building periodic train shutdowns into the life of the plant, it is possible to schedule regular and necessary maintenance on an SOFC train every three years without disturbing production. This maintenance is essential to clean and replace degraded cells to maintain the performance of the overall plant without unwanted shutdowns.

Finally, the NGCC plant (cases 1 and 2) is inferior to that of the SOFC base-load plants with regards to both overall efficiency as

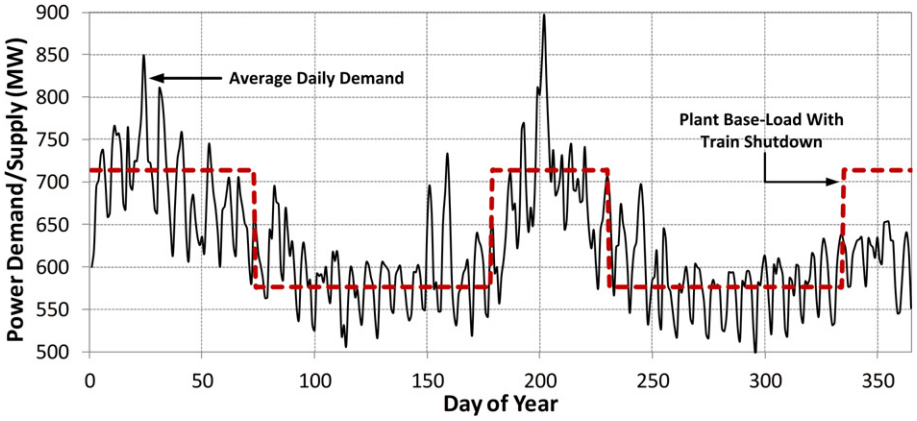

Fig. 6. Average daily demand and base-load plant train shutdown schedule for one simulated year of operation.

Table 4
Simulation and economic results for power generation case studies.

Case	1 NGCC	2 NGCC–CCS	3 SOFC	4 SOFC–CCS	5 SOFC–CAES
Direct fuel usage (tonne yr^{-1})	836,285	972,464	656,332	656,332	656,332
Direct CO_2 emitted (tonne yr^{-1})	2,194,420	219,440	1,722,220	0	1,722,220
Indirect CO_2 emitted (tonne yr^{-1})	47,059	47,059	47,059	47,059	18,991
Total CO_2 emitted (tonne yr^{-1})	2,241,480	266,501	1,769,280	47,059	1,741,210
CO_2 sequestered (tonne yr^{-1})	0	1,974,980	0	1,722,220	0
Electricity generated (MW-h yr^{-1})	6,254,640	6,254,640	6,338,740	6,254,640	6,278,900
Electricity sold (MW-h yr^{-1})	5,345,500	5,345,500	5,360,200	5,345,500	5,427,900
Electrical efficiency[a] (%HHV)	**50.8**	**43.7**	**65.6**	**64.8**	**65.0**
	6 SOFC–CAES–CCS	7 SOFC–TSD	8 SOFC–TSD–CCS	9 SOFC–CAES–TSD	10 SOFC–CAES–TSD–CCS
Direct fuel usage (tonne yr^{-1})	656,332	593,895	593,895	593,895	593,895
Direct CO_2 emitted (tonne yr^{-1})	0	1,558,390	0	1,558,390	0
Indirect CO_2 emitted (tonne yr^{-1})	18,991	117,812	117,812	63,845	63,845
Total CO_2 emitted (tonne yr^{-1})	18,991	1,676,200	117,812	1,622,230	63,845
CO_2 sequestered (tonne yr^{-1})	1,722,220	163,833	1,722,220	163,833	1,722,220
Electricity generated (MW-h yr^{-1})	6,193,000	5,640,700	5,564,640	5,525,100	5,456,200
Electricity sold (MW-h yr^{-1})	5,417,800	5,201,800	5,168,400	5,344,300	5,306,800
Electrical efficiency (%HHV)	**64.1**	**64.6**	**63.7**	**63.2**	**62.4**

[a] Electrical efficiency is calculated as the total power generated by the plant divided by the total HHV fuel input to the plant on a basis of 1 year, whether or not that electricity was actually "sold" to the grid for profit.

well as carbon capture capabilities. Although the NGCC plant has lower capital costs (as will be discussed in Section 3.4) its high fuel consumption, low efficiency and higher CO_2 emission rates are likely to make it less attractive should fuel prices increase and carbon restrictions of some fashion be implemented. For example, case 9 produces about 28% fewer total CO_2 emissions (direct and indirect) than case 1 (NGCC). When CCS is added, the SOFC/CAES plant with train shutdowns (case 10) produces 97% fewer total emissions than case 1 (NGCC), and 76% fewer emissions than case 2 (NGCC with CCS).

3.2. Economic results

The economic results of each of the ten cases examined are presented in Table 5. The LCOE for each case was calculated in the absence and presence of a carbon tax of \$50 $tonne^{-1}$. Due to its very low capital investment, the NGCC plant without CCS is unsurprisingly the most economically attractive configuration without a CO_2 tax and at the current market price of natural gas. However, due to its much lower efficiency and higher fuel utilization than the SOFC base-load plants, it becomes unattractive at a CO_2 tax of \$50 $tonne^{-1}$ or when fuel prices climb to the neighborhood of \$6.16 GJ^{-1} (\$6.50 $MMBtu^{-1}$) [6]. On that note, it is interesting to observe that when no CO_2 incentives are used the addition of CCS to any configuration based around the SOFC results in no more than a 0.08 ¢ kW^{-1} h^{-1} (1.6%) increase in LCOE. This is because a solvent-based CO_2 capture process is not required for the SOFC cases. CCS becomes economically attractive for all processes when a CO_2 tax of \$50 $tonne^{-1}$ is implemented, with the SOFC-based plants having the lowest LCOE.

The increase in capital costs associated with adding a CAES system to the SOFC base-load plant results in a slightly higher LCOE

Table 5
Economic results for each of the plant configurations simulated.

Case	1 NGCC	2 NGCC–CCS	3 SOFC	4 SOFC–CCS	5 SOFC–CAES
Capital cost (\$1,000s)	363,100	718,900	1,212,500	1,239,500	1,373,100
Grid power cost (\$1,000s yr^{-1})	5469	5469	5469	5469	2385
Fuel costs (\$1,000s yr^{-1})	101,800	118,400	79,900	79,900	79,900
CO_2 emission costs[c] (\$1,000s yr^{-1})	112,100	13,300	88,500	2353	87,100
Operating costs[a] (\$1,000s yr^{-1})	16,500	30,400	19,000	19,300	22,500
LCOE[b] (¢ kW^{-1} h^{-1})	**3.57**	**5.04**	**5.00**	**5.07**	**5.29**
LCOE[c] with CO_2 tax (¢ kW^{-1} h^{-1})	**6.084**	**5.335**	**6.967**	**5.123**	**7.206**
	6 SOFC–CAES–CCS	7 SOFC–TSD	8 SOFC–TSD–CCS	9 SOFC–CAES–TSD	10 SOFC–CAES–TSD–CCS
Capital cost (\$1,000s)	1,400,000	1,212,500	1,239,500	1,373,100	1,400,000
Grid power cost (\$1,000s yr^{-1})	2386	11,950	11,950	6880	6880
Fuel costs (\$1,000s yr^{-1})	79,900	72,300	72,300	72,300	72,300
CO_2 emission costs[c] (\$1,000s yr^{-1})	950	83,800	5890	81,100	3190
Operating costs[a] (\$1,000s yr^{-1})	22,500	19,300	19,300	22,500	22,500
LCOE[b] (¢ kW^{-1} h^{-1})	**5.35**	**5.12**	**5.22**	**5.30**	**5.40**
LCOE[c] with CO_2 tax (¢ kW^{-1} h^{-1})	**5.37**	**7.05**	**5.35**	**7.12**	**5.47**

[a] Operating costs include labor, maintenance, catalysts, water consumption, CO_2 transport costs, and materials.
[b] Does not include a CO_2 tax.
[c] Includes a CO_2 tax of \$50 $tonne^{-1}$.

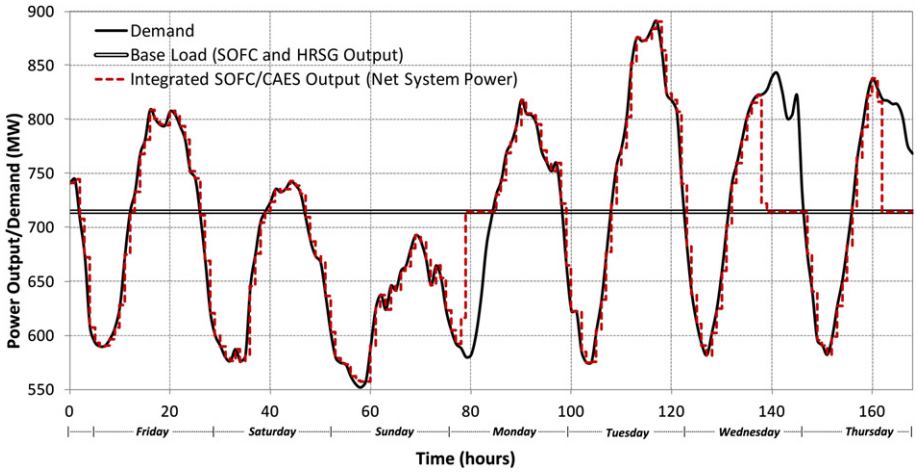

Fig. 7. Simulation results of the SOFC/CAES system for one selected week of operation (June 17–23, 2011). Times in which the output of the SOFC/CAES system matches the base load when demand is less than supply denote times when the cavern is full (at maximum allowable pressure). Times in which the SOFC/CAES system matches the base load when demand exceeds supply denote times when the storage cavern is empty (at minimum allowable pressure).

for the SOFC–CAES cases. However, this slight increase of approximately 0.1 ¢ kW^{-1} h^{-1} (2.0%) allows for much more accurate load-following when CAES is used than the base-load case, and significantly reduces the requirement for additional power being imported from the grid. The addition of train shutdowns, although not advantageous from a purely economic standpoint, reduces the direct fuel consumption cost of the proposed process by approximately 9.5%. Although this may not result in an immediate financial gain, the reduced fuel consumption will result in further fuel cost savings should the price of natural gas increase throughout the lifetime of the plant (see Section 3.4).

Since grid prices are always in flux, the CAES plant provides some protection from unexpected price increases. For example, instead of using the SOFC/CAES hybrid system to minimize load-following mismatch, as was the goal in the present work, one could use the CAES capabilities to maximize profit by storing energy during times of low prices and releasing at higher prices. Although this is left for future work, this property can have significant financial planning and forecasting benefits.

It is important to note that the economic results obtained in this study will be different at different scales, fuel prices, sale prices and other parameters used. For example, smaller system sizes would cause higher LCOEs of both the NGCC and SOFC-based plant designs since the proportion spent on capital increases due to economies-of-scale. For this investigation, our system scale was chosen such that the SOFC/CAES system design is comparable to that of the most reasonable alternative system for bulk power production, namely a modern NGCC plant operating at an output of approximately 700 MW. The effects of variations in many of the other economic parameters are explored in Section 3.4.

3.3. Load-following results and performance

A sample plot of demand and power provided by case 6 (SOFC–CAES–CCS) is given in Fig. 7, and the corresponding cavern pressure profile is displayed in Fig. 8. Table 6 summarizes the load-following metrics used in this investigation for each of the cases examined. It is clear that the CAES-enabled system is able to accurately follow demand above and below the level of the fixed SOFC and HRSG power output during most of the simulated control intervals.

The addition of the CAES component decreases the SSE and WSSE substantially when compared to the SOFC base-plant. From the standpoint of adding the CAES, this makes sense

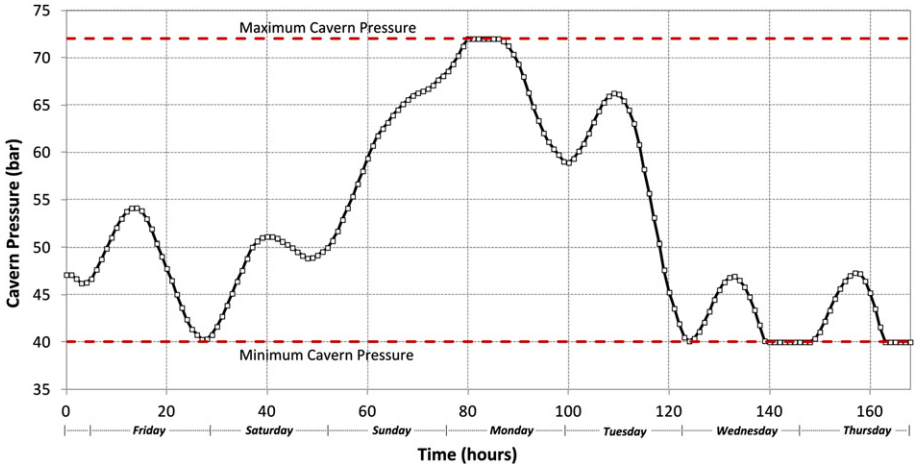

Fig. 8. Pressure profile for one week of simulated operation.

Table 6
Load-following metric results for cases investigated.

Case	Tag	SSE (10^6 [MW-h]^2)	WSSE (10^6 [MW-h]^2)	Relative SSE	Relative WSSE
1	NGCC	162.28	51.73	0.911	0.956
2	NGCC–CCS	162.28	51.73	0.911	0.956
3	SOFC	178.22	54.12	1.000	1.000
4	SOFC–CCS	162.28	51.73	0.911	0.956
5	SOFC–CAES	152.34	42.94	0.855	0.793
6	SOFC–CAES–CCS	135.98	40.13	0.763	0.742
7	SOFC–TSD	84.68	43.45	0.475	0.803
8	SOFC–TSD–CCS	81.95	46.34	0.460	0.856
9	SOFC–TSD–CAES	43.80	24.23	0.246	0.448
10	SOFC–TSD–CAES–CCS	43.70	26.24	0.245	0.485

because the amount over- and under-produced decreases substantially with the addition of load-following capabilities. Train shutdowns also decrease the SSE, and in the final case cause it to be as low as 24.5% of that of the base-load SOFC plant, indicating that the addition of CAES and train shutdowns result in about half as much demand/supply mismatch. For example, when comparing case 5 (SOFC–CAES) to case 9 (SOFC–CAES–TSD), the SSE for case 9 is 28.8% of that of case 5. Similarly to the SSE, the addition of train shutdowns decreases the WSSE, although not by as much. For example, when comparing cases 5 and 9 again, the WSSE for case 9 is 56.5% of that of case 5. This is largely due to the fact that the train shutdowns decrease the amount of overproduction while also slightly increasing the amount of underproduction, the latter of which is penalized more heavily in the WSSE metric. For this reason, the WSSE is likely a better performance metric than SSE; it is most important to meet demand as much as possible, even if over-production is highly wasteful. The only way to improve plant load-following performance with train shutdowns is through the introduction of the CAES plant, which brings the WSSE to 48.5% of the base-load plant when CCS is enabled.

The load-following performance of the CAES-enabled cases is highly dependent on the size of the storage cavern. A sensitivity analysis is shown in Fig. 9 that compares the WSSE of cases 4, 6, 8 and 10. It is clear that increasing the cavern size exhibits diminishing returns with regards to WSSE improvement, and very little improvement for either of cases 6 or 10 is made past 800,000 m^3. There is thus a trade-off to be investigated between increasing cavern sizes for the sake of improved load-following performance and the corresponding increase in capital investment, which is left to future work. The load-following performance of each system is also independent of the base-load system size. Since the demand profiles for the simulations were scaled to the size of the base-load plants investigated, the load-following results (SSE, WSSE, energy storage/withdrawal rates) are equivalent for any reasonable size.

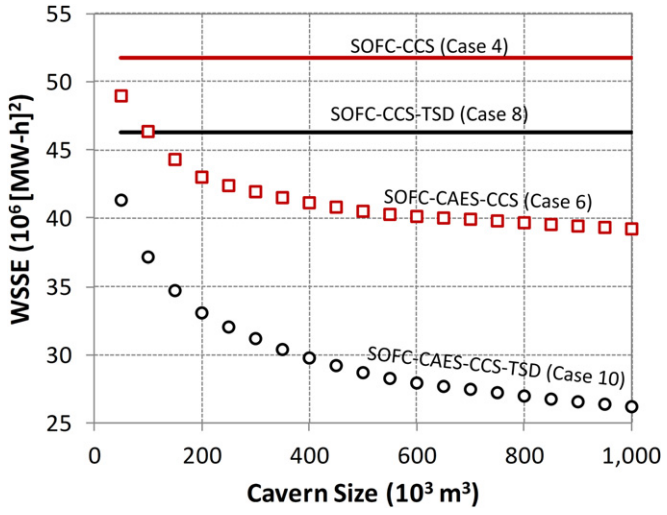

Fig. 9. Effect of cavern size on CCS-enabled system performance.

3.4. Sensitivity analyses

The LCOEs for the cases investigated have been computed as a function of the average lifetime carbon tax paid by the plant and are shown in Fig. 10. This analysis assumes a simple linear CO_2 tax on a per-tonne basis. With the price of natural gas at the current (June 2012) low price of \$2.33 GJ^{-1} (\$2.46 MMBtu^{-1}), it would require a CO_2 tax of \$30 tonne^{-1} to incentivize a system in which CCS is used; anything less would make CCS uneconomical compared to the non-CCS cases. Another interesting observation is that for the parameters investigated in this sensitivity analysis, the addition of CAES at no point becomes the most economical design. However, as mentioned previously, the addition of CAES improves the load-following capabilities of the SOFC base-load plant for a very modest increase in LCOE (only about 5% or 0.3 ¢ kW^{-1} h^{-1}), which is also evident in Fig. 10. SOFC based plants are not economically attractive unless CCS is enabled, where some are significantly less expensive than NGCC with CCS. This is an expected result, since the extremely cost-effective CO_2 capture of an SOFC plant is one of its major advantages in a future of sustainable energy.

Shown in Fig. 11 is a two-dimensional sensitivity map that shows which of the 10 cases has the lowest LCOE based changes in both fuel (natural gas) and CO_2 tax prices. One interesting observation from this plot is that the system of case 10 (SOFC–CAES–CCS–TSD) actually combines to offer the most cost-effective power generation at relatively high gas prices (~\$7.58 GJ^{-1} or \$8 MMBtu^{-1}) and CO_2 taxes (~\$60 tonne^{-1}). As a matter of fact, train shutdown configurations are almost exclusively used above a price of approximately \$7.58 GJ^{-1} (\$8 MMBtu^{-1}), which has occurred several times over the last few decades. Therefore, the CAES and SOFC train shutdown configurations not only protect a plant from sudden increases in fuel and external electricity costs, provide excellent load-following capabilities, reduce wasted energy and resources, and provide the capability to capture essentially 100% of direct CO_2 emissions at only a small cost premium, but it also becomes the outright most economically attractive option in a scenario with high emission taxes and fuel prices. The configuration which is generally the most economically optimal is case 4,

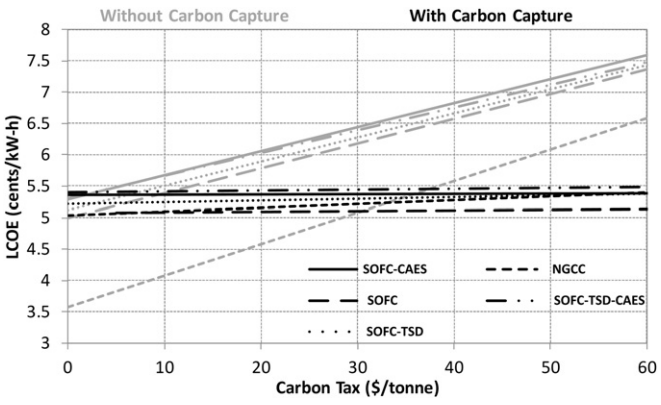

Fig. 10. Effect of CO_2 taxes on LCOE.

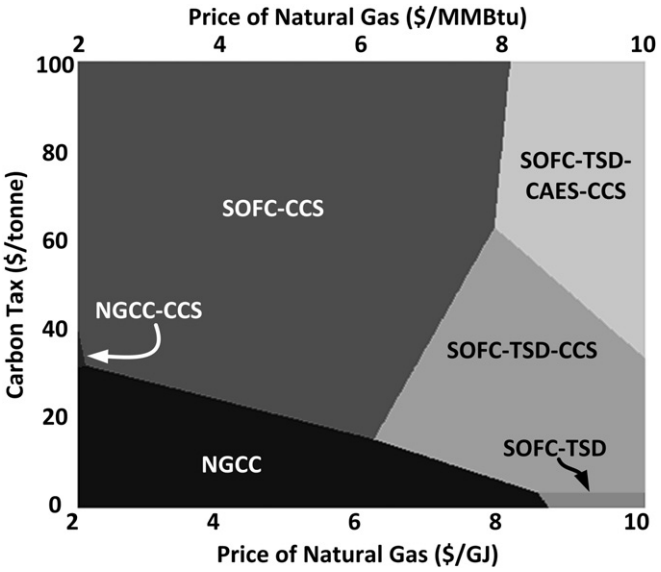

Fig. 11. Sensitivity map of processes exhibiting the lowest LCOE based on natural gas and CO_2 tax prices.

which becomes the most economically feasible with a CO_2 tax of approximately \$30 tonne^{-1} at the current price of natural gas.

4. Conclusions and future work

In this study, the applicability and performance of an integrated SOFC/CAES plant with and without CCS in a load-following power production scenario was investigated. Ten different process configurations were simulated using a combination of Aspen Plus and MATLAB tools. It was found that the addition of CAES to an SOFC plant provided significant load-following capabilities with relatively small penalties to efficiencies (1.1%HHV) and levelized electricity costs (0.08–0.3 ¢ kW^{-1} h^{-1}). The load-following capabilities of the CAES-enabled plants, as measured by the SSE and WSSE metrics, were significantly higher than the base-load cases and were not impacted by the addition of CCS. CCS-enabled configurations using SOFC/CAES strategies were able to reduce direct CO_2 emissions to essentially zero. The introduction of a train shutdown schedule, while useful for maintenance and cleaning purposes, was also found to help reduce fuel consumption with very small penalties to the overall load-following performance of the SOFC/CAES plant.

Overall, the SOFC/CAES process can provide very effective load-following power production with zero direct CO_2 emissions for only a marginal increase in LCOE. Furthermore, SOFC/CAES can be the most economical option should carbon taxes and natural gas prices rise above the range of \$40 tonne^{-1} and \$7.58 GJ^{-1} (\$8 MMBtu^{-1}), respectively. Although SOFCs are perhaps decades away from being implemented on the scale discussed in this study, the forward-looking energy conversion strategy proposed in this work shows great promise for providing future carbon-free peaking power.

Since this is the first known investigation of providing zero-emission peaking power using SOFCs to the best of our knowledge, several simplifying assumptions were made for the sake of this proof-of-concept study. Future work may include the consideration of CAES turbine dynamics, real-time optimization frameworks to maximize plant revenue or profitability (instead of minimizing underproduction and overproduction), market considerations when CO_2 has economic value (such as for enhanced oil recovery), control system considerations, stochastic fuel and material price planning, startup/shutdown penalties of the base load plant (specifically those involved with TSD), and the use of gasified coal, biomass, or other fuel sources instead of or in addition to natural gas. These considerations will likely affect the profitability (whether positively or negatively is unknown at this point) of integrated SOFC/CAES systems.

Nomenclature

Abbreviations

ASU	air separation unit
ATR	auto-thermal reformer
CAES	compressed air energy storage
CCS	carbon capture and sequestration
EOS	equation of state
HHV	higher-heating value
HRSG	heat recovery and steam generation
LCOE	levelized cost of electricity
SOFC	solid oxide fuel cell
SSE	sum of squared error
TSD	train shutdown
WGS	water-gas shift
WSSE	weighted sum of squared error

Mathematical symbols

a	model coefficient
D	demand
F	molar flow rate of air
$\mathcal{F}$	fuel costs
I_M	pseudo-steady-state model intercept
I	capital investment
M	maintenance costs
N	plant lifetime
O	plant over-production
P	pressure in cavern
$\mathcal{P}$	sellable power produced
P_C	compressor pressure at outlet
P_P	net power output of plant
r	discount rate
U	plant under-production
μ	mean
σ	standard deviation

References

[1] H.J. Herzog, D. Golomb, in: C.J. Cleveland (Ed.), Encyclopedia of Energy, Elsevier Science, New York, 2004, pp. 277–287.
[2] US Energy Information Administration, AEO2012 Early Release Outlook, US DOE/EIA- 0383ER (January 2012).
[3] National Energy Board, Canada's Energy Future: Energy Supply and Demand Projections to 2035-Electricity Outlook Highlights. (online). Available HTTP: http://www.neb-one.gc.ca/clf-nsi/rnrgynfmtn/nrgyrprt/nrgyftr/2011/fctsht1134lctrct-eng.html (accessed June 2012).
[4] Energy Information Administration (EIA), Fuel emission factors, Appendix H of instructions to form EIA-1605, U.S. Department of Energy, Washington, DC (online). Available HTTP: http://www.eia.gov/oiaf/1605/pdf/Form%20EIA-1605%20instructions.pdf.
[5] U.S. Environmental Protection Agency (EPA), Inventory of U.S. Greenhouse Gas Emissions and Sinks: 1990–2010. EPA 430-R-12–001, pp. 3–5 (online). Available HTTP: http://www.epa.gov/climatechange/ghgemissions/usinventoryreport.html.
[6] T.A. Adams II, P. Barton, J. Power Sources 195 (2010) 1971–1983.
[7] J. Conti, G.E. Sweetnam, et al., Emissions of Greenhouse Gases in the United States 2007. US DOE/EIA-0573(2007) (December 2008).
[8] M.C. Woods, P.J. Capicotto, J.L. Haslbeck, N.J. Kuehn, M. Matuszewski, L.L. Pinkerton, M.D. Rutkowski, R.L. Schoff, V. Vaysman, Cost and Performance Baseline for Fossil Energy Plants. Volume 1: Bituminous Coal and Natural Gas to Electricity Final Report, DOE/NETL-2007/1281, Revision 1, August 2007.
[9] M.C. Williams, J.P. Strakey, W.A. Surdoval, Int. J. Appl. Ceram. Technol. 2 (2005) 295.

[10] T.A. Trabold, J.S. Lylak, M.R. Walluk, J.F. Lin, D.R. Trojani, Int. J. Hydrogen Energy 37 (2012) 5190.
[11] N.Q. Ming, ECS Trans. 7 (2007) 45.
[12] F.P. Nagel, T.J. Schildhauer, S.M.A. Biollaz, Int. J. Hydrogen Energy 34 (2009) 6809.
[13] E. Achenbach, J. Power Sources 57 (1995) 105–109.
[14] C. Stiller, B. Thorund, O. Bolland, J. Eng. Gas Turbines Power 128 (2006) 551–559.
[15] M. Raju, S.K. Khaitan, Appl. Energy 89 (2012) 474–481.
[16] E. Fertig, J. Apt, Energy Policy 39 (2009) 2330–2342.
[17] H. Hoffeins, Huntorf Air Storage Gas Turbine Power Plant, Energy Supply, Brown Boveri Publication, 1994, DGK 90 202 E.
[18] D.R. Hounslow, W. Grindley, R.M. Louglin, J. Eng. Gas Turbine Power 120 (1988) 875–883.
[19] A. Cavallo, Energy 32 (2007) 120–127.
[20] J.B. Greenblatt, S. Succar, D.C. Denkenberger, R.H. Williams, R.H. Socolow, Energy Policy 35 (2007) 1472–1492.
[21] J. Mason, V. Fthenakis, K. Zweibel, T. Hansen, T. Nikolakakis, Prog. Photovolt. Res. Appl. 16 (8) (2008) 649–668.
[22] S. Succar, R.H. Williams, Compressed Air Energy Storage: Theory, Resources and Applications for Wind Power, Princeton Environmental Institute: Princeton University, 2008.
[23] T.A. Adams II, J. Nease, D. Tucker, P. Barton, Ind. Eng. Chem. Res., in press (2012), http://dx.doi.org/10.1021/ie300996r.
[24] T.S. Lee, J.N. Chung, Y. Chen, Energy Conv. Manage. 52 (2011) 3214–3226.
[25] Independent Electricity System Operator. Ontario Demand and Market Prices. Available HTTP: http://www.ieso.ca/imoweb/siteShared/demand_price.asp?sid=ic (accessed 19.03.12).
[26] F. Mueller, B. Tarroja, J. Maclay, F. Jabbari, J. Brouwer, S. Samuelson, J. Fuel Cell. Sci. Tech. 7 (2010). 031007-1-12.
[27] L. Yang, Y. Weng, J. Power Sources 196 (2011) 3824–3835.
[28] V. Liso, A. Oleson, M. Nielson, S. Kaer, Energy 35 (2011) 4216–4226.
[29] Y. Komatsu, S. Kimijima, J.S. Szmyd, Energy 35 (2010) 982–988.
[30] T. Kuramochi, W. Turkenburg, A. Faaij, Fuel 90 (2011) 958–973.
[31] N. Zhang, N. Lior, J. Eng. Gas Turbines Power 130 (2008) 051701-1–151701-11.
[32] K. Aasberg-Petersen, T.S. Christensen, I. Dybkjær, J. Sehested, M. Østberg, R.M. Coertzen, M.J. Keyser, A.P. Steynberg, in: A. Steynberg, M. Dry (Eds.), Fischer–Tropsch Technology, Elsevier, Amsterdam, 2004.
[33] R. Peters, E. Riensche, P. Cremer, J. Power Sources 86 (2000) 432–441.
[34] K.M. Walters, A.M. Dean, H. Zhu, R.J. Kee, J. Power Sources 123 (2003) 182–189.
[35] R.J. Kee, H. Zhu, A.M. Sukeshini, G.S. Jackson, Combust. Sci. Tech. 180 (2008) 1207–1244.
[36] EG&G Technical Services, DOE/NETL Fuel Cell Handbook, seventh ed., (November 2004).
[37] T.A. Adams II, P.I. Barton, AIChE J. 56 (2010) 3120–3136.
[38] W.L. Luyben, Ind. Eng. Chem. Res. 50 (2011) 13984–13989.
[39] R. Kushnir, Transport Porous Media 73 (2008) 1–20.
[40] Electric Power Research Institute, Wind Power Integration Technology Assessment and Case Studies. EPRI Report 1004806 (2004).
[41] US Energy Information Administration, Fuel Emission Factors (online), U.S. Department of Energy, 2010, Available HTTP: http://www.eia.gov/oiaf/1605/pdf/Form%20EIA-1605%20Instructions.pdf.
[42] US Energy Information Administration, Average utilization of the nation's natural gas combined-cycle power plant fleet is rising (online). Available HTTP: http://www.eia.gov/todayinenergy/detail.cfm?id=1730# (accessed 30.11.11).
[43] K. Branker, M.J.M. Pathak, J.M. Pearce, Renew. Sustain. Energy Rev. 12 (2011) 4470–4482.
[44] W.D. Seider, J.D. Seader, D.R. Lewin, S. Widago, Product and Process Design Principles, third ed., Wiley, Hoboken, NJ, 2009, pp. 534–597.
[45] G. Hossein, Progress in SECA-Based Program. Fuel Cell Energy, Inc. SECA Conference Proceeding, July 26, 2011.
[46] M.C. Williams, J.P. Strakey, W.A. Surdoval, U.S. DOE solid oxide fuel cells: technical advances, in: Proceedings of the 207th Meet. Electrochem. Soc., 2005, p. 1025.
[47] R. Schainker, Compressed Air Energy Storage Cost Analysis, The Electric Power Research Institute, 2009, Report 1016004.
[48] Bloomberg Commodity Prices: Energy. Henry Hub Spot Price of Natural Gas (online). Available HTTP: http://www.bloomberg.com/energy/ (accessed 08.05.12).
[49] D. Lozowski, Chem. Eng. 119 (6) (2012) 80.